THE JOURNAL OF BIOLOGICAL CHEMISTRY VOL. 287, NO. 30, pp. 25631–25639, July 20, 2012

Loss of TMF/ARA160 Protein Renders Colonic Mucus Refractory to Bacterial Colonization and Diminishes Intestinal Susceptibility to Acute Colitis*[S]

Received for publication, March 21, 2012, and in revised form, April 23, 2012 Published, JBC Papers in Press, May 2, 2012, DOI 10.1074/jbc.M112.364786

Shai Bel[‡], Yoav Elkis[‡], Tali Lerer-Goldstein[‡], Abraham Nyska[§], Sally Shpungin[‡], and Uri Nir[‡1]

From [‡]The Mina and Everard Goodman Faculty of Life-Science, Bar-Ilan University, Ramat-Gan 52900, Israel and [§]Sackler School of Medicine, Tel-Aviv University, Tel Aviv 36576, Israel

Background: TMF/ARA160 regulates the NF-κB subunit, p65 RelA, under stress conditions.
Results: Loss of TMF/ARA160 renders mice colonic mucus refractory to bacterial colonization and diminishes intestinal susceptibility to acute colitis.
Conclusion: TMF/ARA160 affects intestinal susceptibility to acute colitis.
Significance: Targeting TMF/ARA160 in the colon may attenuate the onset and progression of acute colitis.

TMF/ARA160 is a Golgi-associated protein with several cellular functions, among them direction of the NF-κB subunit, p65 RelA, to ubiquitination and proteasomal degradation in stressed cells. We sought to investigate the role of TMF/ARA160 under imposed stress conditions *in vivo*. TMF$^{-/-}$ and wild-type (WT) mice were treated with the ulcerative agent dextran sulfate sodium (DSS), and the severity of the inflicted acute colitis was determined. TMF$^{-/-}$ mice were found to be significantly less susceptible to DSS-induced colitis, with profoundly less bacterial penetration into the colonic epithelia. Surprisingly, unlike in WT mice, no bacterial colonies were visualized in colons of healthy untreated TMF$^{-/-}$ mice, indicating the constitutive resistance of TMF$^{-/-}$ colonic mucus to bacterial retention and penetration. Gene expression analysis of colon tissues from unchallenged TMF$^{-/-}$ mice revealed 5-fold elevated transcription of the *muc2* gene, which encodes the major component of the colonic mucus gel, the MUC2 mucin. Accordingly, the morphology of the colonic mucus in TMF$^{-/-}$ mice was found to differ from the mucus structure in WT colons. The NF-κB subunit, p65, a well known transcription inducer of *muc2*, was upregulated significantly in TMF$^{-/-}$ intestinal epithelial cells. However, this did not cause spontaneous inflammation or increased colonic crypt cell proliferation. Collectively, our findings demonstrate that absence of TMF/ARA160 renders the colonic mucus refractory to bacterial colonization and the large intestine less susceptible to the onset of colitis.

TMF/ARA160 is a Golgi-associated protein with various cellular functions. These include a role in retrograde transport processes from endosomes to the Golgi and from the Golgi to the endoplasmic reticulum (1). Additionally, TMF/ARA160 was shown to promote ubiquitination and proteasomal degradation, which is induced in cells subjected to stress insults. The targets of the TMF/ARA160 ubiquitination-promoting activity are key prosurvival transcription factors such as Stat3 and the NF-κB subunit, p65-RelA (2, 3). To gain a deeper insight to the physiological roles of TMF *in vivo*, we established TMF$^{-/-}$ knock-out mice. TMF$^{-/-}$ mice, which lack the TMF protein, develop normally, and are healthy, although the males are infertile due to major sperm maturation defects. These defects could be attributed both to the role of TMF/ARA160 in the transport of Golgi-derived granules to the nuclear apical surface, and to its ubiquitination-promoting activity (4).

Inflammatory bowel disease (IBD)[2] comprises two major chronic inflammatory disorders of the gastrointestinal tract, which can also lead to the development of malignancies of this tissue. These are ulcerative colitis (UC) and Crohn disease (5).

UC develops due to malfunctioning of the colonic mucosal barrier and exposure of epithelial and innate immune cells to the luminal bacterial flora and to bacterial toxins (6, 7). Protection of the large intestine, which harbors an extensive amount (10^{13}–10^{14}) of commensal bacteria, is therefore a formidable challenge. Several components comprise the mucosal/epithelial barrier. These include the extracellular mucus layer facing the lumen, whose main constituent is the evolutionarily preserved glycoprotein MUC2, secreted by the intestinal goblet cells (8). The extracellular barrier is composed of an inner "firmly" adherent mucus layer attached to the intestinal epithelial cell layer and shielding the epithelium from direct contact with bacteria and an outer "loose" non-adherent mucus layer (9). Underneath the firm mucus are the epithelial cell layers which, in addition to the production of mucosal constituents, also serve as an additional barrier restricting the intrusion of pathogens and toxins (10).

Murine models have become essential tools to investigate pathophysiological mechanisms and immunological processes underlying mucosal inflammation, including dextran sodium sulfate (DSS), which when given for a short period induces UC-

* This work was supported by a grant from The Israeli Ministry of Health Chief Scientist Research Foundation.
[S] This article contains supplemental Table 1.
[1] To whom correspondence should be addressed: The Mina and Everard Goodman Faculty of Life Sciences, Bar-Ilan University, Ramat Gan 52900, Israel. Tel.: 972-3-5317794; E-mail: uri.nir@biu.ac.il.

[2] The abbreviations used are: IBD, inflammatory bowel disease; IEC, intestinal epithelial cell; qRT-PCR, quantitative RT-PCR; UC, ulcerative colitis; DSS, dextran sulfate sodium; PCNA, proliferating cell nuclear antigen; KC, chemokine (C-X-C motif) ligand 1.

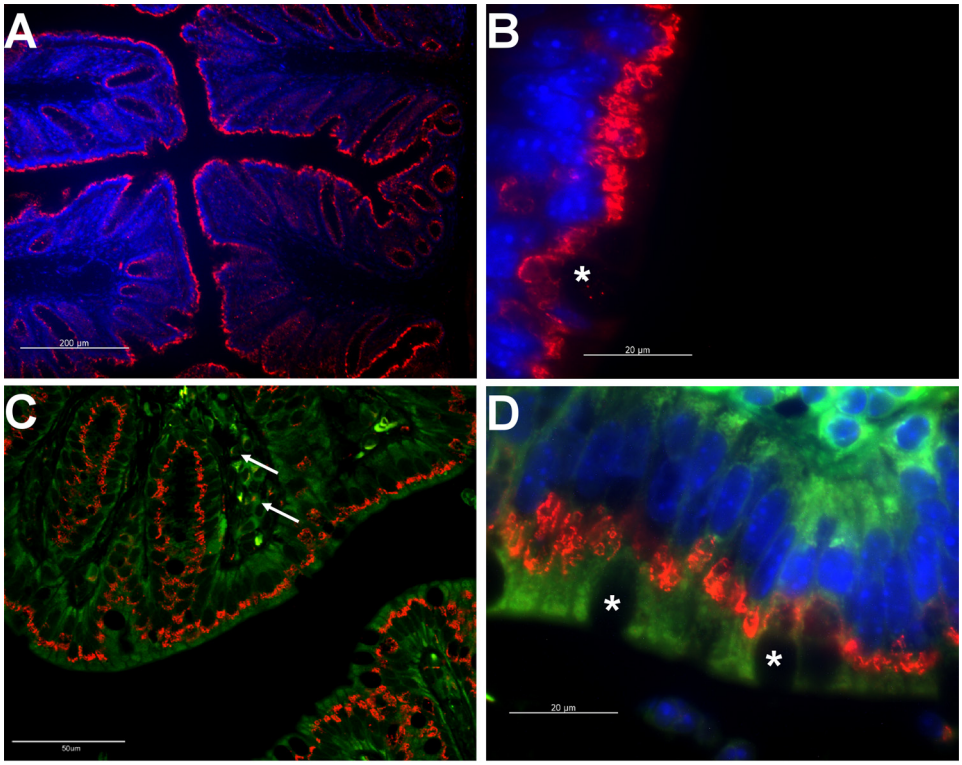

FIGURE 1. **TMF/ARA160 is highly expressed in colonic epithelial columnar cells which face the intestinal lumen.** Shown is an immunofluorescence staining of colon sections from healthy WT mice visualized using fluorescent (*A*, *B*, and *D*) and confocal (*C*) microscopy. Anti-TMF antibody (*red*), Golgi marker (*green*), and Hoechst staining (*blue*) for nuclear visualization show apical localization of TMF/ARA160 exclusively in IECs, including goblet cells (*). *White arrows* in *C* indicate TMF expression in lamina propria cells (*scale bars* are indicated in each image).

like disease in mice (11). DSS is a physical agent with an intrinsic capacity to disrupt the epithelial cell barrier, causing normal mucosal microfloral substances to activate mucosal macrophages, which in turn produce immunomodulatory cytokines and induce acute and chronic inflammatory UC (12).

One of the notions emerging from murine IBD models is that targeted changes in expression of survival factors of intestinal epithelial cells can also affect the vulnerability of this tissue to the induction of inflammatory processes. Accordingly, when the *ikk* gene encoding the NF-κB upstream activator, IKK, is disrupted selectively in intestinal epithelial cells, the intestine becomes extremely sensitive to DSS-induced colitis (13). In agreement with this observation, disruption of the genes encoding either the p50 or p65 (RelA) NF-κB subunits in intestinal epithelial cells, renders these cells sensitive to pathogen and chemically induced cell damage and consequent inflammation (14).

Considering the ability of TMF/ARA160 to direct proteasomal degradation of the NF-κB subunit p65 and the importance of this factor in the onset of IBD, we sought to investigate the potential role of TMF/ARA160 in DSS-induced colitis by testing disease susceptibility of TMF/ARA160 knock-out mice. We show here that the cellular roles of TMF/ARA160 are redundant under normal intestinal functioning in mice but affect intestinal susceptibility to UC. Thus, manipulation of TMF/ARA160 functions could ameliorate intestinal sensitivity to the onset and progression of UC.

MATERIALS AND METHODS

Mice Handling and Maintenance—All experiments were carried out on female, 8-week-old TMF$^{-/-}$ ICR mice (4) and WT littermate controls. Mice were group housed under specific pathogen-free conditions with controlled temperature (25 °C) and photoperiod (12:12 h light/dark cycle) and allowed unrestricted access to standard mouse chow and water. All of the protocols were approved by the Institutional Animal Care and Use Committee at Bar-Ilan University.

Induction of Experimental Colitis—Experimental colitis was induced in mice by administrating 3.0% DSS (molecular mass of 36–50 kDa, MP Biomedicals, Inc.) in water *ad libitum* over a 7-day period. Mice were divided into four groups: 1) DSS-treated WT group, 2) non-treated WT group, 3) DSS-treated TMF$^{-/-}$ group, and 4) non-treated TMF$^{-/-}$ group. Genotype was determined as described previously (4).

Scoring Colitis Clinical Activity—Body weights were measured every other day during the DSS treatment period. Presence of blood in excreta was assessed on the last day of DSS treatment. Disease score was determined as was described previously (15). Mice were sacrificed by cervical dislocation 7 days after induction of colitis. The abdominal cavity was exposed by a midline laparotomy, and the entire colon was removed from the caecum to the anus. The length of the colon was measured, and tissue obtained from each colon was stored at −80 °C and processed for further assays. All measurements were preformed in a blinded fashion.

Histological, Immunohistochemical, and Immunofluorescence Analysis—Colons removed from mice were fixed immediately overnight in either 4% formalin for H&E and immunohistochemical staining or in water-free Methanol-Carnoy's fixative (60% dry methanol, 30% chloroform and 10% acetic

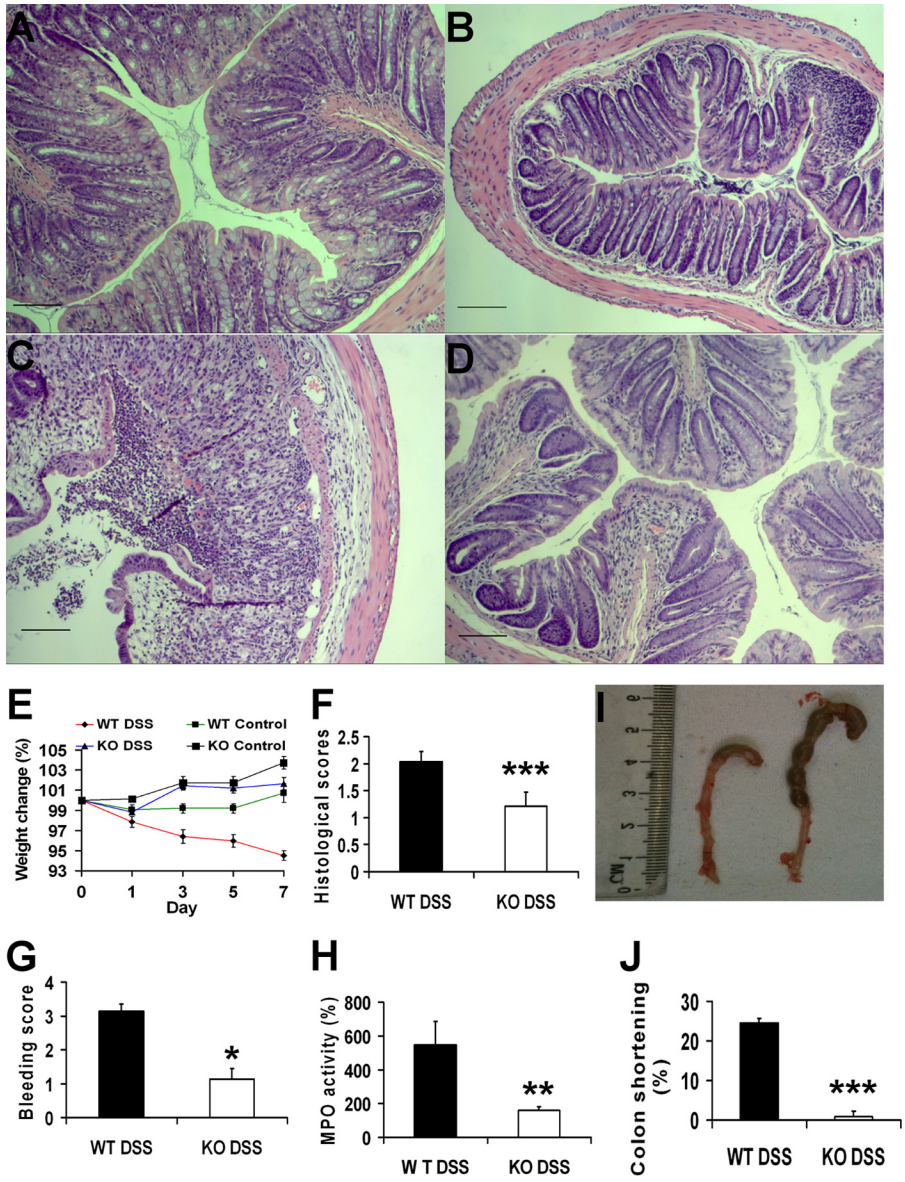

FIGURE 2. **Reduced histopathological and clinical parameters severity of DSS-induced colitis in TMF$^{-/-}$ (KO) mice.** Colon morphology of untreated WT (*A*) and TMF$^{-/-}$ (*B*) mice is shown. Degree of ulceration and loss of crypt architecture in DSS-treated WT (*C*) and TMF$^{-/-}$ (*D*) colons are shown. Images are representative examples of the different groups ($n = 7$ per group). *Scale bars*, 100 μm. Weight loss was presented as mean percent of initial weight ± S.E. (*E*). Histopathological semi-quantitative scores were presented as the mean score (obtained as described under "Materials and Methods") ± S.E. (*F*). Presence of blood in excreta was shown as the mean (determined as described under "Materials and Methods") ± S.E. (*G*). Myeloperoxidase activity was shown as percent change of activity compared with control untreated groups ($n = 7$ per group), reflecting neutrophil infiltrate (*H*). Length of colons from WT DSS-treated (*left*) and KO DSS-treated (*right*) mice are shown (*I*). Colon shortening is represented as mean percent change in colon length of DSS-treated mice compared with untreated mice (*J*) ± S.E. ($n = 7$ per group). *, $p < 0.05$; **, $p < 0.07$; ***, $p < 0.005$.

acid) for 2 h to fix and visualize mucosal bacteria and Mucin2. Fixed tissues were embedded in paraffin and sectioned 4-mm thick, dewaxed using Toluene (Frutarom, Ltd.), and hydrated. For bacterial visualization, sections were stained using a Giemsa stain. For immunohistochemical staining and analysis, antigen retrieval was performed by microwave heating in 0.01 M citric buffer, pH 6. Sections were incubated overnight with the following primary antibodies: anti-TMF1 (1:200) (R02400, clone HPA008729, Sigma-Aldrich), anti-mannosidase II (1:100) (ab24565, Abcam), anti-NF-κB p65 (1:250) (1546-1, EPI Epitomics), anti-Mucin2 (1:200) (sc-15334, H-300, Santa Cruz Biotechnology), and anti-PCNA (1:100) (sc-7907, Santa Cruz Biotechnology). For immunofluorescence analysis, sections were incubated for 1 h with the following secondary antibodies: anti-mouse or anti-rabbit Alexa Fluor 488 and anti-rabbit Alexa Fluor 594 (1:150) (Molecular Probes, Invitrogen), and the nuclei were stained with 0.1 g/ml Hoechst (Sigma-Aldrich). For HRP immunohistochemistry, a secondary anti-rabbit HRP-conjugated antibody was used according to the manufacturer's instructions (ab80437, Abcam). Nuclei were visualized with hematoxylin (Sigma-Aldrich).

Histological Assessment of Colitis—Histopathological analysis and semi-quantitative scoring was performed by a board-certified toxicological pathologist according to the scoring system described by Cooper *et al.* (16), taking into consideration the grades of extension (laterally, along the mucosa and deep

into the mucosa, submucosa, and/or muscular layers) of the inflammation and ulceration. Analysis was performed in a blinded fashion.

Myeloperoxidase Activity—Neutrophil infiltration into the colon was quantified by measuring myeloperoxidase activity according to the technique described by Boughton-Smith *et al.* (17). Results are shown as percent change in kinetics compared with control mice.

Fluorescent in Situ Hybridization—Paraffin sections were dewaxed with toluene and hybridized with a general bacterial probe, EUB 338, conjugated to FITC as described by Johansson *et al.* (9). Nuclei were stained with 0.1 g/ml Hoechst (Sigma-Aldrich).

Quantification of Colonic Bacteria—DNA isolation from colons was performed using DNeasy® blood and tissue kit (Qiagen) according to the manufacturer's instructions. A total of 100 ng of DNA was analyzed by PCR for 23 cycles as described by Yan *et al.* (18). PCR amplification of the GAPDH gene was performed to ensure equal loading. Gels were analyzed for a density plot histogram using NIH ImageJ software.

RNA Isolation and Quantitative Real-time PCR Analysis—RNA from colon tissue was extracted using TRI reagent (Molecular Research Center, ICN) following the manufacturer's instructions. Total RNA (1 μg) was reverse-transcribed using SuperScript first-strand synthesis system for qRT-PCR (Invitrogen). Quantitative real-time PCR was performed using the StepOnePlus system with Fast SYBER Green Master Mix and analyzed with StepOne software (Applied Biosystems). Expression levels were normalized to GAPDH and are presented as fold expression change relative to untreated wild-type samples. The primers used are shown in supplemental Table S1.

NF-κB p65 RelA Transcription Factor Activity Assay—Isolation of nuclear extracts from mouse colons and NF-κB p65 binding activity assay were performed using the NF-κB (p65) transcription factor assay kit (Cayman Chemical) according to the manufacturer's instructions.

Statistical Analysis—Data are presented as mean values ± S.E. Statistical analysis was conducted using the Student's *t* test and is indicated for each figure. The *n* for each experiment is noted in the figure legend.

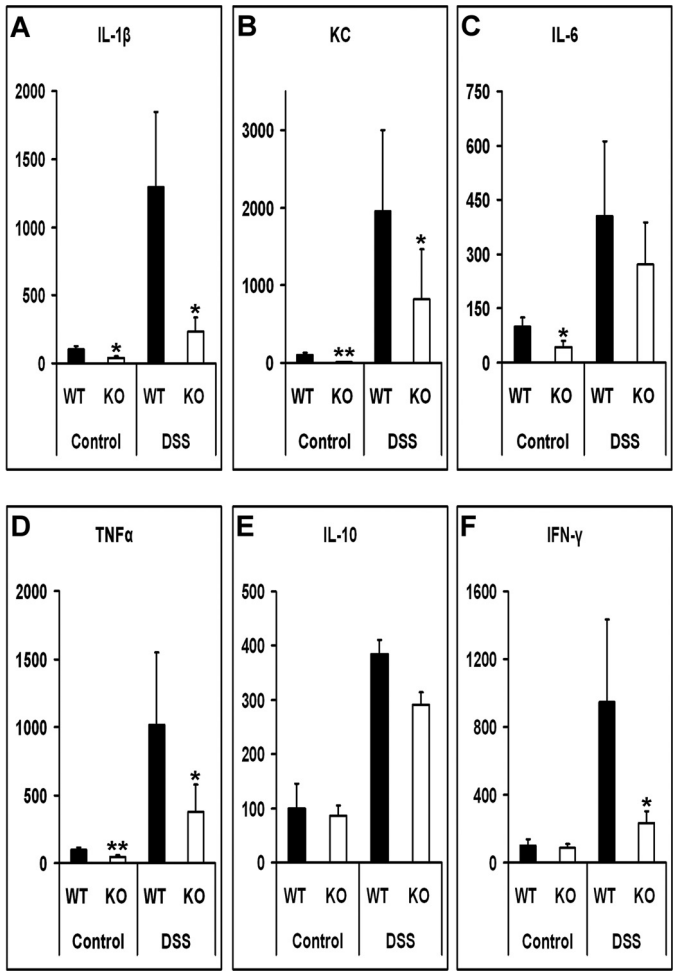

FIGURE 3. **Reduced expression of cytokines and proinflammatory mediators in control and DSS-treated TMF$^{-/-}$ (KO) mice.** Shown is a real-time qRT-PCR analysis of mRNAs encoding cytokines and proinflammatory mediators in untreated (control) and DSS-treated (DSS) WT and KO mice. Obtained levels were normalized to GAPDH mRNA and are presented as mean percent change in mRNA levels as compared with WT control mice ± S.E. ($n = 5$ per group). *, $p < 0.05$; **, $p < 0.01$.

RESULTS

TMF Is Highly Expressed in Apical Cytoplasm of Intestinal Epithelial Cells—TMF/ARA160 has been shown previously to reside in the Golgi apparatus of several mammalian cell lines (1). It was also demonstrated that TMF/ARA160 is abundantly expressed in most murine tissues, with remarkably high levels in the colon (4). To investigate the localization of TMF/ARA160 in the mouse colon, immunofluorescent staining was performed on tissue sections. Staining was almost exclusive to intestinal epithelial cells (IEC) of all types: enterocytes, goblet cells, and crypt stem cells (Fig. 1, *A* and *B*). In these cells, TMF/ARA160 localized to the apical cytoplasm (Fig. 1, *A* and *B*). Utilizing confocal microscopy, we found that TMF does not co-localize with the Golgi apparatus and appears scattered in the apical cytoplasm of enterocytes (Fig. 1, *C* and *D*). In the lamina propria, TMF/ARA160 is expressed at relatively low levels and is concentrated in a defined area in the cytoplasm of these cells (Fig. 1*C*)

TMF$^{-/-}$ Mice Are Less Sensitive to Chemically Induced Colitis—Pathological examination of colon tissue sections from female TMF$^{-/-}$ mice of all ages show normal architecture of the colonic epithelium and the interior lamina propria (Fig. 2, *A* and *B*). These results demonstrate that lack of TMF/ARA160 does not cause pathological effects in unchallenged mice colon.

To assess the role of TMF/ARA160 under injury and inflammation in the colon, we used the established model of DSS-induced colitis. WT and TMF$^{-/-}$ littermates, at the age of 8 weeks, were administered 3% DSS in drinking water, and control mice were given drinking water without additives. After 7 days, mice were sacrificed, and tissue samples were collected for further processing and examination. Histopathological inspection revealed significantly less tissue damage and ulceration in TMF$^{-/-}$ colons as opposed to their WT littermates (Fig. 2, *C*, *D*, and *F*). Other symptoms of colitis such as weight loss, fecal blood, and colon shortening were also diminished in TMF$^{-/-}$-treated mice (Fig. 2, *E*, *G*, *I*, and *J*). To evaluate the extent of

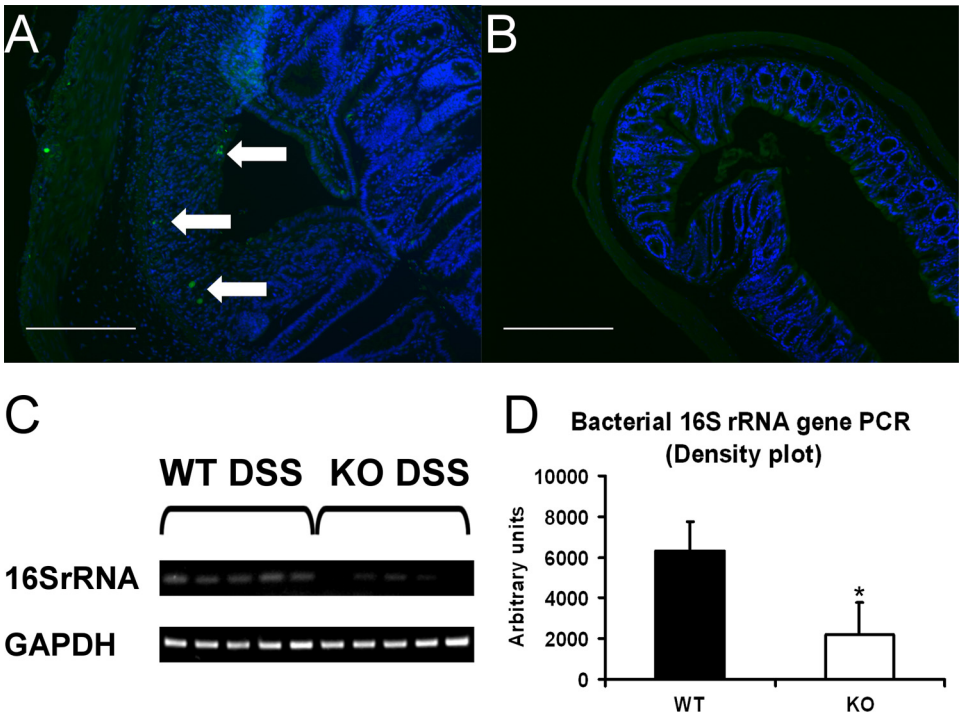

FIGURE 4. **Reduced bacterial infiltration in colonic tissue of DSS-treated TMF$^{-/-}$ (KO) mice.** Fluorescent *in situ* hybridization with a specific probe directed toward the 16 S bacterial RNA was used to visualize bacterial penetration into colonic tissue from DSS-treated WT (*A*) and KO (*B*) mice ($n = 5$ per group). Bacteria (*green*) are indicated by *arrows* shown against nuclear (*blue*) counter stain (*scale bars*, 200 μm). Shown is a semi-quantitative PCR analysis of the bacterial 16 S rRNA gene using 100 ng of DNA isolated from DSS-treated WT and KO colons (*C*), and a density plot histogram presentation (*D*) of the gel in *C* ± S.E. PCR amplification of GAPDH is shown to ensure equal loading ($n = 5$ per group). *, $p < 0.005$.

neutrophil infiltration into the mucosa, we measured myeloperoxidase activity in tissue extracts. Although myeloperoxidase levels in WT mice were elevated ~5-fold following DSS treatment, as expected, TMF$^{-/-}$ treated mice showed only a 2-fold increase in myeloperoxidase activity, relative to their untreated controls (Fig. 2*H*).

The difference in inflammatory scores between DSS treated WT and TMF$^{-/-}$ mice was further manifested by the differences between the expression levels of key proinflammatory agents in the two cohorts. Using qRT-PCR analysis, we showed that the levels of mRNAs encoding IL-1β, KC, and TNFα are significantly lower in TMF$^{-/-}$ mice. Notably, although the levels of the above three cytokines were lower in colons of both untreated and DSS-treated TMF$^{-/-}$ mice, the level of the IFNγ transcript was decreased significantly only in colons of DSS-treated TMF$^{-/-}$ animals (Fig. 3).

To further evaluate the damage to the epithelial barrier following DSS treatment, we analyzed the colonic tissue sections for bacterial penetration by fluorescent *in situ* hybridization using a general, bacterial-specific 16 S rRNA probe. Although bacteria were abundant in colonic tissues of DSS-treated WT mice, only weak staining was observed in TMF$^{-/-}$-treated animals (Fig. 4, *A* and *B*). Accordingly, semi-quantitative PCR analysis using primers directed toward the highly conserved bacterial 16 S rRNA gene sequence confirmed these results, showing significantly lower bacterial presence in the colons of DSS-treated TMF$^{-/-}$ mice (Fig. 4, *C* and *D*). These results suggest that the lack of TMF in the IEC diminishes barrier disruption and inflammatory damage under conditions of induced acute colitis.

Bacterial Colonies Are Not Detected in Colonic Mucus of TMF$^{-/-}$ Mice—We postulated that the diminished susceptibility of TMF$^{-/-}$ mice to DSS induced colitis could result from greater epithelial barrier integrity, which decreases bacterial penetration upon DSS treatment (19). Considering our observation that bacterial penetration of the colonic mucosal layer was diminished significantly in DSS-treated TMF$^{-/-}$ mice, we sought to investigate the ability of bacterial cells to colonize the colonic mucus of untreated TMF$^{-/-}$ mice. We used a very rapid and aggressive fixation technique, the Carnoy's fixation, which was proven to preserve the mucus layer and its inhabiting bacteria (8). Giemsa differential staining was applied to visualize the bacterial cells. In colons of untreated WT mice, bacterial colonies clearly were visible colonizing the mucus layer. Surprisingly, no bacterial colonies were visible in sections of colon samples from untreated TMF$^{-/-}$ mice (Fig. 5, *A–D*). To confirm and quantify our observations, we used semi-quantitative PCR analysis of the 16 S rRNA gene sequence present in colons of untreated WT and TMF$^{-/-}$ mice. This showed significantly lowered bacterial presence in colons of TMF$^{-/-}$ mice (Fig. 5, *E* and F). Thus, absence of TMF/ARA160 renders the colonic mucus refractory to bacterial colonization.

Elevated Expression of muc2 mRNA and Distinct Architecture of Colonic Mucus in TMF$^{-/-}$ Mice—The colonic mucus layers are major constituents of the colonic barrier. Although the firm inner layer physically separates the gut bacteria from the epithelial cell layer, the loose outer layer allows bacterial adherence (20). The decreased bacterial colonization could therefore reflect modified characteristics of the colonic mucus in TMF$^{-/-}$ mice.

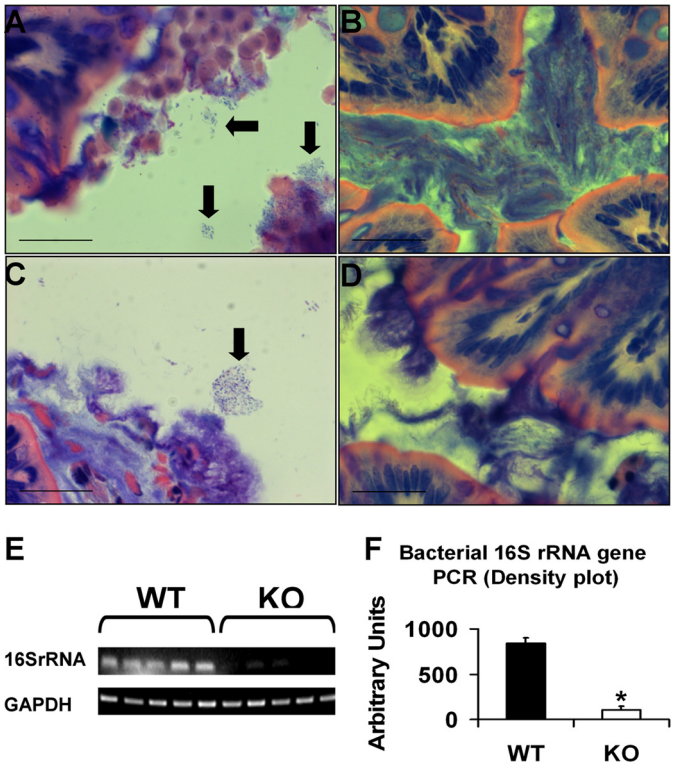

FIGURE 5. **Bacterial colonies are not detected in colonic lumen and mucosa of untreated TMF$^{-/-}$ (KO) mice.** Colons of untreated WT (*A* and *C*) and KO (*B* and *D*) mice were fixed with Carnoy's fixative and stained with Giemsa. Bacterial colonies in WT colons are indicated by *arrows*. No bacterial colonies are visible in colons from untreated KO mice. Images are representative examples of the different groups ($n = 5$ per group). *Scale bars*, 20 μm. Shown is a semi-quantitative PCR analysis of the bacterial 16 S rRNA gene using 100 ng DNA isolated from untreated colons (*E*), and density plot histogram presentation (*F*) of the gel in *E* ± S.E. PCR amplification of GAPDH is shown to ensure equal loading ($n = 5$ per group). *, $p < 0.0005$.

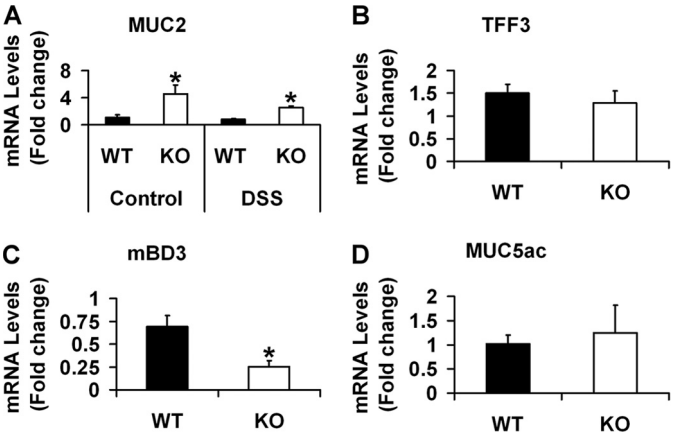

FIGURE 6. **Increased *muc2* mRNA levels in colons of TMF$^{-/-}$ (KO) mice.** Shown is a real-time qRT-PCR analysis of *muc2* mRNA encoding the MUC2 mucin from untreated (control) and DSS-treated (DSS) WT and KO mice (*A*). Levels of *tff3* mRNA encoding the intestinal epithelial repair factor TFF3 (*B*), of the *mbd3* mRNA encoding the antimicrobial protein mBD3 (*C*), and of *muc5ac* mRNA encoding the MUC5AC mucin (*D*) were determined in colons of untreated WT and KO mice. Expression levels were normalized to GAPDH and are presented as mean change in mRNA levels as compared with WT control mice ± S.E. ($n = 5$ per group). *. $p < 0.05$.

To validate this notion, we analyzed the expression of an indispensable component of mucosal protective function, the *muc2* gene, which is expressed exclusively in goblet cells and encodes the key colonic mucus component, the MUC2 gel-forming mucin (21). By use of real-time qRT-PCR analysis, we found a 5-fold increase in the *muc2* mRNA level in colons of untreated TMF$^{-/-}$ mice comparing to untreated WT mice, and this increase was maintained after DSS treatment as well (Fig. 6*A*).

Another plausible cause of the decreased bacterial penetration to the colonic mucosal layer of DSS-treated TMF$^{-/-}$ mice is the overexpression of antibacterial intestinal peptides of the defensin family (22). However, gene expression analysis in TMF$^{-/-}$ mice did not reveal any increase in the levels of mRNAs encoding the antimicrobial peptide mBD3 or the trefoil family protein TFF3 (Fig. 6, *B* and C), which is thought to maintain colonic epithelium stability (23). Similarly, qRT-PCR analysis of *muc5ac* mRNA, encoding the MUC5AC mucin, which has been shown to attenuate parasitic pathogen infiltration (24), showed no significant variance between WT and KO mice (Fig. 6*D*).

The significant increase in *muc2* mRNA level in colonic epithelium of untreated TMF$^{-/-}$ mice suggests altered characteristics of the colonic mucus in these animals. To investigate this notion, we used Carnoy's fixation, which preserves the mucus layer architecture. Colonic sections were stained with specific Mucin2 antibody to visualize the colonic mucus morphology. As expected (8), staining of colon sections from WT mice showed a thin and densely stained firm inner layer overlaid by a diffuse loose outer mucosal layer (Fig. 7, *A* and *C*). However, in colonic sections from TMF$^{-/-}$, we found a uniform, thick, and dense mucus layer (Fig. 7, *B* and *D*).

Up-regulation of NF-κB p65 RelA Activity in IEC of TMF$^{-/-}$ Mice—One of the known transcription activators of the *muc2* gene is the transcription factor, NF-κB, which has been shown to be targeted to proteasomal degradation by TMF/ARA160 (2, 26). Specific immunohistochemical staining revealed a major increase in the protein levels of the p65 NF-κB subunit in the IECs of untreated TMF$^{-/-}$ mice (Fig. 8, *A* and *B*). To examine whether the increased level of the p65 protein leads to an up-regulation of NF-κB activity, the DNA-binding activity of the NF-κB p65 subunit was determined in colons of untreated WT and TMF$^{-/-}$ mice using a commercial NF-κB p65 transcriptional activity assay kit. This revealed a 2-fold increase in the relative level of NF-κB p65 transcriptional activity in TMF$^{-/-}$ mice (Fig. 8*E*). The NF-κB transcription regulatory activity was shown to be crucial for colonic epithelial integrity by regulating anti apoptotic genes in IECs (13). We therefore examined mRNA levels of the survival gene *bcl-xl*, which is a downstream target of NF-κB p65 (10). Real-time qRT-PCR analysis revealed a 2-fold increase in the *bcl-xl* mRNA level in colons of untreated TMF$^{-/-}$ mice in comparison with colons of untreated WT mice (Fig. 8*F*). Because NF-κB has been shown to control expression of proteins with anti-apoptotic and pro-proliferative activities (13), we examined whether the increase in NF-κB p65 activity leads to an excessive proliferation of TMF$^{-/-}$ IECs. Immunohistochemical staining of PCNA, a marker of cell proliferation (28), did not show any difference in PCNA-positive cells in colonic crypts of untreated WT *versus* TMF$^{-/-}$ mice (Fig. 8, *C* and *D*).

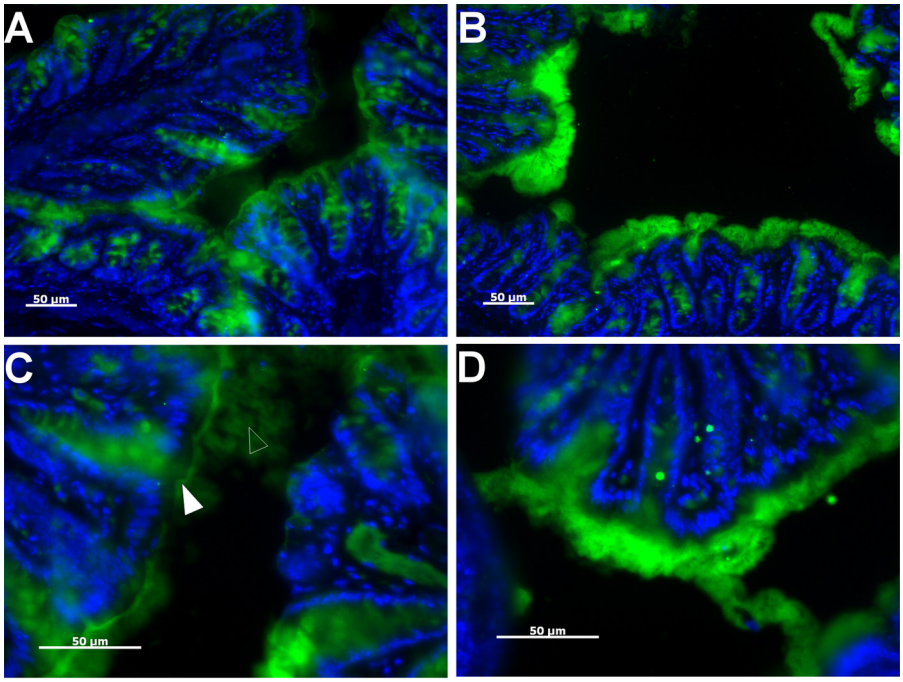

FIGURE 7. **Distinct mucus morphology in colons of untreated TMF$^{-/-}$ (KO) mice.** Shown is an immunofluorescent staining of MUC2 in colon sections from untreated WT (*A* and *C*) and KO (*B* and *D*) mice ($n = 5$ per group). Anti-MUC2 antibody (*green*), combined with Hoechst staining (*blue*) for nuclear visualization was used to visualize the morphology of the narrow firm (*filled arrowhead*) and wide loose (*empty arrowhead*) mucus layers in WT mice in contrast to the uniform thick dense mucus layer in KO mice. *Scale bars*, 50 μm.

DISCUSSION

Ulcerative colitis is an IBD, which combines impaired host reaction to commensal bacteria with ulcerative outcomes. This results mainly from the malfunctioning of the colonic mucosal barrier, thereby enabling the exposure of the innate immune cells residing in the colonic lamina propria to the luminal bacterial flora and to bacterial toxins (7, 9). Consequent production of inflammatory cytokines initiates inflammatory cascades that lead to colonic tissue damage and to chronic inflammation, which can initiate malignant transformation (29).

In the current study, we show that the TMF/ARA160 protein affects the susceptibility of the colon to the onset of acute colitis. Absence of TMF/ARA160 alleviates the pathoclinical and inflammatory parameters that characterize and define the onset and progression of DSS-induced acute colitis. Because one of these parameters is bacterial penetration of the colonic tissue (30), which is a key step in the development of UC, we investigated whether the mucosal barrier of the colons in TMF$^{-/-}$ mice exhibits distinct properties from those of the WT mucosal barrier. Surprisingly, we found that although bacterial colonies inhabit the mucosal layer in colons of WT mice, no bacterial colonies could be detected in the mucus and epithelial layers in colons of TMF$^{-/-}$ mice. Accordingly, usage of quantitative methods revealed a significantly decreased amount of bacteria in TMF$^{-/-}$ colons in comparison with WT mice. Thus, absence of TMF/ARA160 renders the colonic mucus layer less available to bacterial retention and penetration, and consequently to bacterial colonization.

The refractory nature of TMF$^{-/-}$ colonic mucus to bacterial colonization suggests a change in its properties, which could be linked either to elevated accumulation of anti-microbial substances (31) or to increased viscosity (32), reflecting a modification in its biochemical composition. Gene expression analysis revealed an elevated expression of the *muc2* gene, encoding the gel-forming MUC2 mucin, in colons of TMF$^{-/-}$ mice. The increased accumulation of MUC2 may thereby affect the biochemical and biophysical characteristics of the TMF$^{-/-}$ colonic mucus. In compliance with this notion, we noticed distinct architecture of the colonic mucus in TMF$^{-/-}$ mice. Although the WT mucus appeared as expected (8) to be composed of a thin, firm inner layer overlaid by a diffuse, loose outer layer, the TMF$^{-/-}$ mucus primarily exhibited only one dense and thick layer. Further biochemical analysis is required for confirming that the uniform colonic mucus of TMF$^{-/-}$ mice bears the physical characteristics of the inner firm layer of WT colons. However, the morphological structure observed by the MUC2 staining, combined with the lack of bacterial colonies support our postulated notion. The pivotal role of MUC2 and the colonic mucus layer in protection from the onset of IBD was underscored previously by the severe colonic inflammation, which develops spontaneously in MUC2-deficient mice (33). Furthermore, the lowered levels of the murine cytokine KC and of the antibacterial peptide mBD3, which are produced in response to microbial stimuli (34, 35), coincide with the observation that bacterial presence is significantly lower in colons of TMF$^{-/-}$ mice.

TMF/ARA160 was shown previously to direct the proteasomal degradation of the NF-κB subunit, p65 (2). Immunostaining of colonic sections from TMF$^{-/-}$ mice demonstrated an increased accumulation of NF-κB p65 in TMF$^{-/-}$ IECs, and functional assay documented the up-regulation of the NF-κB p65 transcription inducing activity in the TMF$^{-/-}$ colon. Because NF-κB was shown to activate the transcription of the *muc2* gene (5, 6), we propose that absence of TMF/ARA160

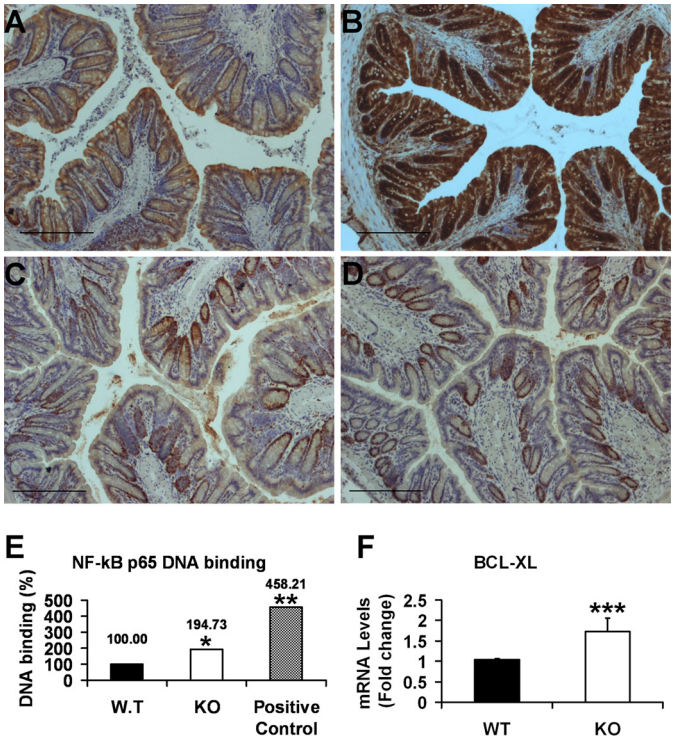

FIGURE 8. **Up-regulation of the NF-κB subunit p65-RelA in untreated colonic epithelium of TMF$^{-/-}$ (KO) mice.** Shown is an immunohistochemical staining of NF-κB p65 in colon sections from untreated WT (*A*) and KO (*B*) mice. PCNA-positive cells indicate the proliferation levels of IEC in colons of untreated WT (*C*) and KO (*D*) mice. Images are representative of the different groups ($n = 6$ per group). *Scale bars*, 200 μm. Nuclear extracts from colons of untreated WT and KO mice were analyzed for NF-κB p65 transcriptional activity via DNA binding by ELISA (*E*). Results are represented as percent change from WT mean level ± S.E. ($n = 5$). A real-time qRT-PCR analysis of *bxl-xl* mRNA encoding the Bcl-x_L anti-apoptotic protein is shown (*F*). Expression levels were normalized to GAPDH and are presented as mean change in mRNA levels as compared with WT control mice ± S.E. ($n = 5$ per group). *, $p < 0.0001$; **, $p < 0.001$; ***, $p < 0.05$.

increases the levels of transcription factors that up-regulate the expression of the *muc2* gene. This leads to the elevated accumulation of MUC2, to altered structure and characteristics of the colonic mucus, and to its consequent diminished availability for bacterial colonization. Thus, the mucus of TMF$^{-/-}$ mice renders the colonic mucosa a more robust barrier to bacterial penetration and to the onset of colitis. Although this alteration does not affect the normal development and growth of the animals, it does provide them with reduced sensitivity to the onset of acute colitis.

NF-κB is a well known modulator of inflammation as well as a survival factor (13). However, recent studies have shown that elevated basal levels of NF-κB activity in IECs does not necessarily lead to the onset of inflammation and even has a protective effect in the onset of acute colitis (25, 27). Our results show that in colons of TMF$^{-/-}$ mice, the elevated level of NF-κB p65 activity does not induce spontaneous inflammation or elevated cytokine production. Moreover, we cannot exclude the possibility that other factors such as elevated accumulation of the prosurvival protein Bcl-x_L, driven by NF-κB in TMF$^{-/-}$ IECs (14), also contribute to the reduced intestinal susceptibility of TMF$^{-/-}$ mice to DSS-induced acute colitis. Further studies should extend our understanding of the entire regulatory network, which is governed by TMF/ARA160 and could affect the susceptibility of mammals to IBD.

REFERENCES

1. Yamane, J., Kubo, A., Nakayama, K., Yuba-Kubo, A., Katsuno, T., Tsukita, S., and Tsukita, S. (2007) Functional involvement of TMF/ARA160 in Rab6-dependent retrograde membrane traffic. *Exp. Cell Res.* **313,** 3472–3485
2. Abrham, G., Volpe, M., Shpungin, S., and Nir, U. (2009) TMF/ARA160 down-regulates proangiogenic genes and attenuates the progression of PC3 xenografts. *Int. J. Cancer* **125,** 43–53
3. Perry, E., Tsruya, R., Levitsky, P., Pomp, O., Taller, M., Weisberg, S., Parris, W., Kulkarni, S., Malovani, H., Pawson, T., Shpungin, S., and Nir, U. (2004) TMF/ARA160 is a BC-box-containing protein that mediates the degradation of Stat3. *Oncogene* **23,** 8908–8919
4. Lerer-Goldshtein, T., Bel, S., Shpungin, S., Pery, E., Motro, B., Goldstein, R. S., Bar-Sheshet, S. I., Breitbart, H., and Nir, U. (2010) TMF/ARA160: A key regulator of sperm development. *Dev. Biol.* **348,** 12–21
5. Podolsky, D. K. (2002) Inflammatory bowel disease. *N. Engl. J. Med.* **347,** 417–429
6. Forbes, E., Murase, T., Yang, M., Matthaei, K. I., Lee, J. J., Lee, N. A., Foster, P. S., and Hogan, S. P. (2004) Immunopathogenesis of experimental ulcerative colitis is mediated by eosinophil peroxidase. *J. Immunol.* **172,** 5664–5675
7. Ohtake, K., Koga, M., Uchida, H., Sonoda, K., Ito, J., Uchida, M., Natsume, H., and Kobayashi, J. (2010) Oral nitrite ameliorates dextran sulfate sodium-induced acute experimental colitis in mice. *Nitric Oxide* **23,** 65–73
8. Johansson, M. E., Larsson, J. M., and Hansson, G. C. (2011) The two mucus layers of colon are organized by the MUC2 mucin, whereas the outer layer is a legislator of host-microbial interactions. *Proc. Natl. Acad. Sci. U.S.A.* **108,** 4659–4665
9. Johansson, M. E., Phillipson, M., Petersson, J., Velcich, A., Holm, L., and Hansson, G. C. (2008) The inner of the two Muc2 mucin-dependent mucus layers in colon is devoid of bacteria. *Proc. Natl. Acad. Sci. U.S.A.* **105,** 15064–15069
10. McGuckin, M. A., Eri, R., Simms, L. A., Florin, T. H., and Radford-Smith, G. (2009) Intestinal barrier dysfunction in inflammatory bowel diseases. *Inflamm. Bowel Dis.* **15,** 100–113
11. Strober, W., Fuss, I. J., and Blumberg, R. S. (2002) The immunology of mucosal models of inflammation. *Annu Rev. Immunol.* **20,** 495–549
12. Kitajima, S., Takuma, S., and Morimoto, M. (1999) Changes in colonic mucosal permeability in mouse colitis induced with dextran sulfate sodium. *Exp. Anim.* **48,** 137–143
13. Wullaert, A., Bonnet, M. C., and Pasparakis, M. (2011) NF-κB in the regulation of epithelial homeostasis and inflammation. *Cell Res.* **21,** 146–158
14. Steinbrecher, K. A., Harmel-Laws, E., Sitcheran, R., and Baldwin, A. S. (2008) Loss of epithelial RelA results in deregulated intestinal proliferative/apoptotic homeostasis and susceptibility to inflammation. *J. Immunol.* **180,** 2588–2599
15. Araki, A., Kanai, T., Ishikura, T., Makita, S., Uraushihara, K., Iiyama, R., Totsuka, T., Takeda, K., Akira, S., and Watanabe, M. (2005) MyD88-deficient mice develop severe intestinal inflammation in dextran sodium sulfate colitis. *J. Gastroenterol.* **40,** 16–23
16. Cooper, H. S., Murthy, S. N., Shah, R. S., and Sedergran, D. J. (1993) Clinicopathologic study of dextran sulfate sodium experimental murine colitis. *Lab. Invest.* **69,** 238–249
17. Boughton-Smith, N. K., Wallace, J. L., and Whittle, B. J. (1988) Relationship between arachidonic acid metabolism, myeloperoxidase activity, and leukocyte infiltration in a rat model of inflammatory bowel disease. *Agents Actions* **25,** 115–123
18. Yan, Y., Laroui, H., Ingersoll, S. A., Ayyadurai, S., Charania, M., Yang, S., Dalmasso, G., Obertone, T. S., Nguyen, H., Sitaraman, S. V., and Merlin, D. (2011) Overexpression of Ste20-related proline/alanine-rich kinase exacerbates experimental colitis in mice. *J. Immunol.* **187,** 1496–1505
19. Petersson, J., Schreiber, O., Hansson, G. C., Gendler, S. J., Velcich, A., Lundberg, J. O., Roos, S., Holm, L., and Phillipson, M. (2011) Importance and regulation of the colonic mucus barrier in a mouse model of colitis.

Am. J. Physiol. Gastrointest. Liver Physiol. **300,** G327–333
20. Saleh, M., and Elson, C. O. (2011) Experimental inflammatory bowel disease: Insights into the host-microbiota dialog. *Immunity* **34,** 293–302
21. Bergstrom, K. S., Kissoon-Singh, V., Gibson, D. L., Ma, C., Montero, M., Sham, H. P., Ryz, N., Huang, T., Velcich, A., Finlay, B. B., Chadee, K., and Vallance, B. A. (2010) Muc2 protects against lethal infectious colitis by disassociating pathogenic and commensal bacteria from the colonic mucosa. *PLoS Pathog.* **6,** e1000902
22. Cunliffe, R. N., and Mahida, Y. R. (2004) Expression and regulation of antimicrobial peptides in the gastrointestinal tract. *J. Leukoc Biol.* **75,** 49–58
23. Kalabis, J., Rosenberg, I., and Podolsky, D. K. (2006) Vangl1 protein acts as a downstream effector of intestinal trefoil factor (ITF)/TFF3 signaling and regulates wound healing of intestinal epithelium. *J. Biol. Chem.* **281,** 6434–6441
24. Hasnain, S. Z., Evans, C. M., Roy, M., Gallagher, A. L., Kindrachuk, K. N., Barron, L., Dickey, B. F., Wilson, M. S., Wynn, T. A., Grencis, R. K., and Thornton, D. J. (2011) Muc5ac: A critical component mediating the rejection of enteric nematodes. *J. Exp. Med.* **208,** 893–900
25. Eckmann, L., Nebelsiek, T., Fingerle, A. A., Dann, S. M., Mages, J., Lang, R., Robine, S., Kagnoff, M. F., Schmid, R. M., Karin, M., Arkan, M. C., and Greten, F. R. (2008) Opposing functions of IKKβ during acute and chronic intestinal inflammation. *Proc. Natl. Acad. Sci. U.S.A.* **105,** 15058–15063
26. Ahn, D. H., Crawley, S. C., Hokari, R., Kato, S., Yang, S. C., Li, J. D., and Kim, Y. S. (2005) TNF-α activates MUC2 transcription via NF-κB but inhibits via JNK activation. *Cell Physiol. Biochem.* **15,** 29–40
27. Guma, M., Stepniak, D., Shaked, H., Spehlmann, M. E., Shenouda, S., Cheroutre, H., Vicente-Suarez, I., Eckmann, L., Kagnoff, M. F., and Karin, M. (2011) Constitutive intestinal NF-κB does not trigger destructive inflammation unless accompanied by MAPK activation. *J. Exp. Med.* **208,** 1889–1900
28. Xu, G., Ren, G., Xu, X., Yuan, H., Wang, Z., Kang, L., Yu, W., and Tian, K. (2010) Combination of curcumin and green tea catechins prevents dimethylhydrazine-induced colon carcinogenesis. *Food Chem. Toxicol.* **48,** 390–395
29. Kraus, S., and Arber, N. (2009) Inflammation and colorectal cancer. *Curr. Opin. Pharmacol.* **9,** 405–410
30. Johansson, M. E., Gustafsson, J. K., Sjöberg, K. E., Petersson, J., Holm, L., Sjövall, H., and Hansson, G. C. (2010) Bacteria penetrate the inner mucus layer before inflammation in the dextran sulfate colitis model. *PLoS One* **5,** e12238
31. Kim, Y. S., and Ho, S. B. (2010) Intestinal goblet cells and mucins in health and disease: Recent insights and progress. *Curr. Gastroenterol. Rep.* **12,** 319–330
32. Swidsinski, A., Sydora, B. C., Doerffel, Y., Loening-Baucke, V., Vaneechoutte, M., Lupicki, M., Scholze, J., Lochs, H., and Dieleman, L. A. (2007) Viscosity gradient within the mucus layer determines the mucosal barrier function and the spatial organization of the intestinal microbiota. *Inflamm. Bowel Dis.* **13,** 963–970
33. Van der Sluis, M., De Koning, B. A., De Bruijn, A. C., Velcich, A., Meijerink, J. P., Van Goudoever, J. B., Büller, H. A., Dekker, J., Van Seuningen, I., Renes, I. B., and Einerhand, A. W. (2006) Muc2-deficient mice spontaneously develop colitis, indicating that MUC2 is critical for colonic protection. *Gastroenterology* **131,** 117–129
34. Shea-Donohue, T., Thomas, K., Cody, M. J., Aiping Zhao, Detolla, L. J., Kopydlowski, K. M., Fukata, M., Lira, S. A., and Vogel, S. N. (2008) Mice deficient in the CXCR2 ligand, CXCL1 (KC/GRO-α), exhibit increased susceptibility to dextran sodium sulfate (DSS)-induced colitis. *Innate Immun.* **14,** 117–124
35. Rivas-Santiago, C. E., Rivas-Santiago, B., León, D. A., Castañeda-Delgado, J., and Hernández Pando, R. (2011) Induction of β-defensins by l-isoleucine as novel immunotherapy in experimental murine tuberculosis. *Clin. Exp. Immunol.* **164,** 80–89